macromol

MDPI

Article

Relationships Between Composition, Microstructure, Rheology, and Functional Performance in Carbopol-Based Emulgels and Bigels

Sonya Tsibranska-Gyoreva [1,2,*], Petya Peneva [3], Yana Gvozdeva [3,4,5], Nadya Politova-Brinkova [2], Margarita Kassarova [5] and Slavka Tcholakova [1]

[1] Department of Chemical and Pharmaceutical Engineering, Faculty of Chemistry and Pharmacy, Sofia University, 1164 Sofia, Bulgaria; sc@lcpe.uni-sofia.bg
[2] Centre of Competence "Sustainable Utilization of Bio-Resources and Waste of Medicinal and Aromatic Plants for Innovative Bioactive Products" (BIORESOURCES BG), 1504 Sofia, Bulgaria; np@lcpe.uni-sofia.bg
[3] Department of Pharmaceutical Technology and Biopharmacy, Faculty of Pharmacy, Medical University of Plovdiv, 15A Vasil Aprilov Blvd., 4002 Plovdiv, Bulgaria; petya.peneva@mu-plovdiv.bg (P.P.); yana.gvozdeva@mu-plovdiv.bg (Y.G.)
[4] Research Institute at Medical University of Plovdiv (RIMU), 4002 Plovdiv, Bulgaria
[5] Center for Competence "PERIMED-2", BG16RFPR002-1.014-0007, Medical University of Plovdiv, 4002 Plovdiv, Bulgaria
* Correspondence: st@lcpe.uni-sofia.bg

Abstract

This study investigates composition-microstructure-rheology-performance relationships in Carbopol-based emulgels and bigels containing different oils. Optical microscopy revealed polydisperse droplets in liquid paraffin, isopropyl myristate, and almond oil formulations, whereas cetyl alcohol systems exhibited larger, irregular birefringent particles with Maltese cross-like patterns. All formulations showed shear-thinning behavior and predominantly elastic responses ($G' > G''$). Cetyl alcohol-based emulgels exhibited higher elastic moduli and viscosity than those containing other oils. Increasing Carbopol concentration from 0.5% to 1% enhanced elasticity and viscosity, while reducing viscosity losses during heating from 10 to 40 °C from 35 to 40% to 11–26%. Bigels containing 20% and 30% oleogel exhibited elastic moduli approximately 20% and 80% higher than the hydrogel, respectively, suggesting possible synergistic mechanical reinforcement. Correlation analysis revealed relationships between rheological parameters, drug release, and spreadability. Viscosities above approximately 150 Pa·s were associated with reduced drug release, while moderate viscosity favored a balance between structural integrity, spreadability, and release performance. The absence of visible changes after 12 months of storage was consistent with temperature-ramp rheology results, suggesting potential use as a preliminary screening tool for formulation stability. Overall, oil phase selection, phase structuring, and Carbopol concentration enable tailoring stable and functional emulgel and bigel formulations for pharmaceutical and cosmetic applications.

Keywords: emulgels; bigels; rheology; drug release; spreadability

Check for updates

Academic Editor: Loic Hilliou

Received: 17 September 2026
Revised: 18 October 2026
Accepted: 27 October 2026
Published: 31 October 2026

Copyright: © 2026 by the authors. Licensee MDPI, Basel, Switzerland. This article is an open access article distributed under the terms and conditions of the Creative Commons Attribution (CC BY) license.

1. Introduction

Topical drug delivery systems offer localized therapeutic action with minimal systemic side effects. Among these, multiphase gel-based dispersion systems such as emulgels and bigels have emerged as versatile vehicles combining the advantages of emulsions and gels or oleogels and hydrogels, respectively, in terms of skin feel, stability, drug loading/delivery,

patient compliance and release profile [1–3]. Therefore, in recent years, such formulations have been intensively developed as a platform for dermal application of various drugs [4–6] and compounds of natural origin [7–9]. Beyond topical application, systems such as bigels could also be utilized in the food industry to preserve probiotic activity and to replace saturated and trans fats in meat products (e.g., sausages), baked goods, confectionery, and dairy products without compromising their texture [10–12]. Recent advances in semi-solid dosage forms have seen significant growth driven by the integration of nanotechnology, "smart" polymers, and advanced rheological control methods. These innovations successfully overcome traditional limitations regarding penetration of the skin barrier (stratum corneum) [12–16]. The primary advancement enabled by nanotechnology is the reduction in oil droplet size to 10–200 nm. This drastically increases the specific surface area, improves release kinetics, and allows the drug to penetrate deeper skin layers without the need for aggressive chemical penetration enhancers [17].

Emulgels and bigels are modern biphasic semi-solid systems that combine the advantages of gels with liquid or structured lipid phases for dermal, buccal, and transdermal application.

A part of the main advantages of emulgels and bigels in the pharma and cosmetic industry is related to their ability to include both hydrophilic and lipophilic active substances, as well as their potential usage in controlled drug delivery [18,19]. This is due to their specific composition: emulgels typically consist of an emulsion phase incorporated within a gel matrix, whereas bigels are formed by blending hydrogel and oleogel networks in different ratios. In this sense, the distinct internal architecture of these systems could impart unique mechanical and rheological properties potentially influencing their performance, stability, and user acceptance. Therefore, discovering the differences in the properties of emulgels and the respective bigels would contribute to the overall understanding and improvements in the area of their applications. The rheological behavior of emulgels and bigels depends strongly on their composition and internal structure. Both systems typically exhibit shear-thinning and viscoelastic behavior, while bigels may exhibit higher elastic moduli and mechanical strength due to the presence of two structured phases and their interactions [20]. Their drug release characteristics also depend on the distribution of the active substance between the phases and the internal organization of the formulation. In some systems, the structured hydrogel and oleogel phases may provide additional resistance to drug diffusion, resulting in prolonged release compared with conventional emulgels [21,22]. The presence of structured phases may also improve physical stability; however, both emulgels and bigels can undergo destabilization processes, including phase separation, depending on their composition and storage conditions [23].

Despite their immense potential for drug delivery, emulgels and bigels face a number of technological and biopharmaceutical limitations related to phase instability and long-term stability. Furthermore, striking a balance between rheological properties and drug efficacy is a major challenge; while high viscosity and a dense polymer network ensure excellent skin retention, they also create significant resistance to diffusion. This drastically slows the rate at which the drug substance is released and permeates the skin barrier. Scaling up production presents another challenge, as parameters such as shear sensitivity, temperature, and air bubble formation are difficult to control when preparing large quantities of semi-solid formulations. Despite growing scientific interest, a comprehensive theoretical model for predicting the behavior and functionality of these systems remains lacking due to their complex microstructure [12,24,25].

The comparative investigations of emulgels and the respective bigels reported in the literature, however, are few [26–29] and have primarily focused on systems based on gelatin or poloxamer.

Sagiri et al. [26] investigated bigels, made with stearate organogel and gelatin, and showed that bigels possess better mucoadhesive and mechanical properties, being more elastic and firmer than emulgels. Rheological tests reported by Satapathy et al. [27] for gelatin-based sesame oil-containing emulgels and bigels confirmed these differences: bigels' higher firmness was linked to instantaneous force upon loading, while their significant viscous component, estimated via stress relaxation, was related to structural rearrangement. Furthermore, bigels based on gelatin–agar hydrogel and soybean oil organogel investigated by Wakhet et al. [28], consistently showed the highest impedance compared to emulgels and pure hydrogels. Despite these differences in mechanical and electrical properties, Wakhet et al. [28] found similar swelling and drug release profiles between the two types of formulations. Mazurkevičiūtė et al. [29] studied the effect of oil incorporation methods on poloxamer-based formulations containing ciclopirox olamine, comparing emulgels and a bigel. They found that gelating the oil phase significantly improved the mechanical properties of the formed bigel. However, all tested formulations (emulgels with and without polysorbate 80, and the bigel) exhibited similar antifungal activity. The authors also advised that adding an emulsifier is necessary when mixing the poloxamer gel with mineral oil to create a thermally stable semi-solid emulgel. Given the limited research mainly confined to gelatin and poloxamer systems, a significant gap remains in comparing emulgels and bigels using other gelling agents or oils.

The gelling agents, actually, are very important for the appropriate consistency of the biphasic systems like emulgels and bigels. Among the various gelling agents, Carbopol (a crosslinked polyacrylic acid polymer) is frequently used due to its excellent thickening, stabilizing, and bioadhesive properties [30] and finds application in different pharmaceutical formulations, including these of controlled-release type [31,32].

Additionally, the choice of oils in the emulgels and bigels plays a crucial role in the respective drug delivery, skin feel, and stability [19,21,33–37]. For instance, bigels containing fish oil or almond oil have been shown to enhance the transdermal delivery of drugs like imiquimod and ketoprofen due to the oil's unique fatty acid composition, which aids skin permeation [19,33]. The choice and concentration of the oil also impact sensory attributes; formulations with higher lipophilic phase proportions (35–40%) can feel greasy, which is often undesirable for users [34], whereas emulgels are typically known for their favorable, non-greasy feel [21]. The oil type also contributes to the physical stability of emulgels by affecting droplet size and polymer interactions, with one study finding that andiroba oil offered better stability than passion fruit or sweet almond oil [36]. The oil's melting point can even influence the freeze–thaw stability of gelled emulsions relevant to frozen foods [37]. While traditional accelerated aging tests at high temperatures are used for long-term stability assessment of cosmetic and pharmaceutical products [38,39], temperature-ramp rheology has been explored as a complementary approach for assessing temperature-dependent structural changes and identifying potential signs of instability [40,41].

The viscoelastic properties and rheology of semi-solid topical formulations are critical as they directly influence applicability, spreadability, drug release, and patient compliance [42,43]. While many studies only provide steady shear and viscosity data [8,44], this is insufficient for fully characterizing complex systems like emulgels and bigels; a more in-depth analysis of viscoelastic properties using oscillating tests (amplitude, frequency, and temperature ramps) is necessary. The current literature has limited studies on the viscoelastic properties of emulgels and bigels [35,43], and there is a significant gap regarding comprehensive comparative rheological profiling of respective emulgels and bigels, especially concerning the influence of varying oil chemistry and concentration. To address this, previous research by the authors focused on plant-oil-based bigels (Carbopol hydrogel/sorbitan monostearate-almond oil-based organogel) [45] and later investigated

the influence of different oil phases and gelling agent concentrations on Carbopol-based emulgels [46] identified an almond oil-based emulgel with low Carbopol concentration as having maximum drug release, prolonged therapeutic effect, and high stability over six months, suggesting a potential correlation between lower viscosity and drug release and therapeutic efficiency, which highlights the need to further explore the relationship between therapeutic performance and visco-elasticity.

This study continues previous research [45,46] to provide a comprehensive understanding of Carbopol-based bigels and emulgels, focusing on their rheological viscoelastic properties, microstructure, and long-term stability. The work systematically evaluates emulgels containing four different oils (liquid paraffin, cetyl alcohol, isopropyl myristate, and almond oil) to compare the effects of plant-based versus synthetic oils. Combining optical microscopy with four rheological tests—steady shear, frequency sweep, amplitude sweep, and temperature ramp—the study offers a full characterization suite. This approach aims to address key literature gaps by (1) directly comparing how the structural differences between emulgels and bigels affect viscoelasticity and mechanical integrity, (2) systematically exploring how oil chemistry and concentration modulate emulgel rheology, and (3) assessing temperature-dependent rheological behavior as a complementary approach to conventional stability testing. The novel aspects of this work relate to providing a comprehensive characterization of the rheological behavior and microstructure of emulgels and bigels. This knowledge is valuable for a better understanding of the relationship between microstructure, rheological behavior, and functionality and would contribute to the development of a comprehensive theoretical model for predicting the behavior and functionality of these systems.

2. Materials and Methods

2.1. Materials

This study utilized analytical-grade Carbopol® 940 (The Lubrizol Corporation, Wickliffe, OH, USA), propylene glycol (PG; Sigma-Aldrich, St. Louis, MO, USA), ethanol 95% (*v*/*v*), Span® 60 (Sigma-Aldrich, USA), Tween® 60 (Sigma-Aldrich, USA), light liquid paraffin (LLP; Ph. Eur.), cetyl alcohol (CA; Sigma-Aldrich, USA), isopropyl myristate (IPM; Sigma-Aldrich, USA), almond oil (AO), triethanolamine (TEA), and purified water.

Sodium dodecyl sulfate (SDS, product of Acros Organics, Geel, Belgium, cat. No: 23042-500) was used in some optical observations as a dilution medium for the concentrated formulations.

2.2. Methods

2.2.1. Preparation of Emulgels and Bigels

A detailed description of the methods for emulgels preparation is reported in a previous study [46]. Briefly, the oil, containing LLP (at different concentrations between 5 and 7.5% *w*/*w*), CA, IPM or AO with the dissolved Span 60, and the hydrophilic phase, containing PG, Tween 60, ethanol and purified water, were heated to the temperature of 70–80 °C. The oil and aqueous phases were heated to 70–80 °C to ensure complete melting of the solid lipophilic components (Span 60 and, where applicable, CA), facilitate homogeneous mixing, and maintain consistent emulsification conditions across all formulations. The oil phase was then added to the hydrophilic phase under continuous stirring (300 rpm). Carbopol dispersions with concentrations of 1% and 2% (*w*/*w*) were prepared in purified water at room temperature under continuous stirring (300 rpm). The obtained emulsions were then mixed with the corresponding Carbopol dispersions at a 1:1 weight ratio, resulting in final Carbopol concentrations of 0.5% and 1% (*w*/*w*), respectively. Subsequently, the pH was adjusted to 5.5–6.5 using TEA. All formulations were drug-free.

The investigated bigels were prepared by mixing a Carbopol-based (1% *w*/*w*) hydrogel (containing also 5% *w*/*w* PG, 10% *w*/*w* ethanol (95% *v*/*v*) and 84% *w*/*w* purified water) and an organogel containing 85% *w*/*w* almond oil and 15% *w*/*w* Span 60. The hydrogel was prepared at 25 °C at 400 rpm as TEA was added (pH 5.5–6.5), and the organogel was obtained at 60 °C at 100 rpm. The heated organogel was added to the hydrogel under continuous stirring at 500 rpm in ratios 20:80 and 30:70 (*w*/*w*), and consecutive cooling to ambient temperature was applied, obtaining formulations BG20 and BG30, respectively.

The composition of the various emulgel and bigel formulations with the respective concentrations of the components is presented in Table 1.

Table 1. Composition of the studied emulgels and bigels (% *w*/*w*).

Formulation Code	Carbopol 940	LLP	CA	IPM	AO	Span® 60	Tween® 60	PG	Ethanol	Purified Water
C1_LLP5	1	5	-	-	-	0.69	1.31	5	10	q.s.
C1_LLP6	1	6	-	-	-	0.69	1.31	5	10	q.s.
C1_LLP7.5	1	7.5	-	-	-	0.69	1.31	5	10	q.s.
C1_CA5	1	-	5	-	-	0.14	1.86	5	10	q.s.
C1_IPM5	1	-	-	5	-	0.69	1.31	5	10	q.s.
C1_AO5	1	-	-	-	5	0.69	1.31	5	10	q.s.
C0.5_LLP5	0.5	5	-	-	-	0.69	1.31	5	10	q.s.
C0.5_LLP6	0.5	6	-	-	-	0.69	1.31	5	10	q.s.
C0.5_LLP7.5	0.5	7.5	-	-	-	0.69	1.31	5	10	q.s.
C0.5_CA5	0.5	-	5	-	-	0.14	1.86	5	10	q.s.
C0.5_IPM5	0.5	-	-	5	-	0.69	1.31	5	10	q.s.
C0.5_AO5	0.5	-	-	-	5	0.69	1.31	5	10	q.s.
BG20	0.8	-	-	-	17	3	-	4	8	q.s.
BG30	0.7	-	-	-	25.5	4.5	-	3.5	7	q.s.

The detailed bigel preparation procedure was reported in a previous work [45].

After preparation of the studied models, physical examination of the emulgels and bigels was carried out. The prepared emulgels and bigels were visually inspected for their color, homogeneity, consistency, and phase separation. It was found that all formulations were white, viscous and creamy with a smooth and homogeneous texture. The consistency of all emulgels was suitable for dermal application. No phase separation was observed as a sign of physical instability.

2.2.2. Optical Observations

The droplet shape in the examined samples was determined by optical observations in transmitted or cross-polarized light using a microscope Axio Imager M2m (Zeiss, Germany).

In these experiments we investigated either the concentrated formulations or samples diluted with a 5 mM SDS solution. The samples were diluted with a 5 mM SDS solution to facilitate the visualization of individual droplets and reduce the risk of coalescence during dilution, which could otherwise occur when using pure water due to the decrease in surfactant concentration in the continuous phase. The studied formulations were observed as being placed on a glass slide between three microscope glass cover slips.

The droplet size distributions were determined by quantitative analysis of optical microscopy images. At least 500 droplets were analyzed for each formulation. The Sauter mean diameter (d_{32}) and volume-weighted mean diameter (d_{43}) were calculated as follows:

$$d_{32} = \Sigma(n_i d_i^3)/\Sigma(n_i d_i^2)$$

$$d_{43} = \Sigma(n_i d_i^4)/\Sigma(n_i d_i^3)$$

where n_i is the number of droplets with diameter d_i. The polydispersity index (PDI) was calculated as the ratio d_{43}/d_{32}, with higher values indicating broader droplet size distributions. Droplet size analysis was not performed for cetyl alcohol-containing formulations due to the irregular morphology of the dispersed particles, which prevented reliable determination of their diameters.

2.2.3. Rheological Measurements

The rheological properties of the investigated emulgels and bigels were characterized by using a rotational rheometer, Discovery Hybrid Rheometer DHR-3 (TA instruments, New Castle, DE, USA). For all experiments we used a parallel plate geometry with a diameter of 40 mm. Two types of oscillatory shear tests as well as steady shear deformation and temperature ramp rheological measurements were performed to characterize the viscoelastic properties and the temperature response of the samples. To mimic the conditions of application of the studied emulgels and bigels on the skin, the first three types of tests were performed at 32 °C (typical skin body temperature). In these cases, the samples were loaded and an equilibration step was applied for 300 s at T = 32 °C. Afterwards the frequency sweeps, the amplitude sweeps and the steady shear experiments were performed with each sample. The particular parameters of the measurements are presented in the following Section Frequency Sweeps, Section Amplitude Sweeps and Section Steady Shear. The temperature ramp experiments were performed with a separate sample as explained below in Section Temperature Ramp Tests.

Frequency Sweeps

In these tests the oscillation frequency was varied logarithmically between 0.01 and 100 Hz. The storage (elastic) and the loss (viscous) moduli, G′ and G″, respectively, were measured as a function of the frequency of oscillations at a constant amplitude of deformation ($\gamma_A \approx 1\%$). The selected strain values were chosen based on preliminary amplitude sweep measurements to ensure that all subsequent oscillatory experiments were performed within the linear viscoelastic region.

Amplitude Sweeps

The oscillation strain amplitude, γ_A, was varied logarithmically from 0.05 to 500% at a fixed frequency of 1 Hz. Again, the elastic, G′, and viscous, G″, moduli of the formulations were determined as a function of strain amplitude.

Steady Shear

The viscosity of the samples was measured in flow ramp experiments, in which the shear rate, $\dot{\gamma}$, was logarithmically varied between 0.001 s^{-1} and 2000 $s^{-1,}$ and the shear stress was measured.

Temperature Ramp Tests

In these tests, the temperature was raised from 10 °C to 40 °C with a heating rate of 5 °C/min while the sample was sheared at a fixed shear rate, $\dot{\gamma}$, of 1 s^{-1}. The shear stress was

measured and the viscosity was determined as a function of temperature. To homogenize the sample, we first performed a pre-shear at a fixed shear rate, $\dot{\gamma}$, of 20 s^{-1} at T = 10 °C before the temperature ramp test was performed.

2.2.4. Long-Term Stability Tests

Independent stability tests were performed with the studied emulgel and bigel formulations based on observations of the change in the systems' visual appearance upon storage. These assessments were performed in accordance with the International Council for Harmonisation guidelines. For these experiments the emulgels were packed in tightly closed plastic containers and stored at 30 ± 2 °C/65 ± 5% RH. After 12 months of storage, evaluation of the visual appearance of the samples was performed.

3. Results and Discussion

3.1. Optical Microscopy Observations

Optical observations of concentrated emulgels revealed dispersed entities of irregular shape (Figure 1). Liquid paraffin samples showed small liquid drops (Figure 1A), while isopropyl myristate and almond oil samples had larger, more polydisperse drops, some of which exhibited partial coalescence (red arrows, Figure 1D). In contrast, the cetyl alcohol-containing emulgel exhibited larger dispersed particles with a distinct morphology (Figure 1B). Dilution with 5 mM SDS clarified the phase behavior. The IPM and AO emulgels formed spherical drops (Figure 1G,H), suggesting Span 60 is well-solubilized in the oil phase. In contrast, the LLP emulgel drops remained slightly deformed (Figure 1E), likely due to a solid shell of Span 60 that had adsorbed on the drop surface and frozen. Most notably, dilution of the CA-containing emulgels revealed birefringent dispersed particles exhibiting Maltese cross-like patterns under cross-polarized light (Figure 1F). In addition, concentric optical features were observed around some particles, particularly in the formulation with the lower Carbopol concentration (Figure S1). These observations are consistent with the possible formation of onion-like lamellar structures, as previously reported for similar systems [47–49]. However, since such birefringent patterns may also arise from other anisotropic structures, additional structural characterization would be required to confirm the presence of an onion phase.

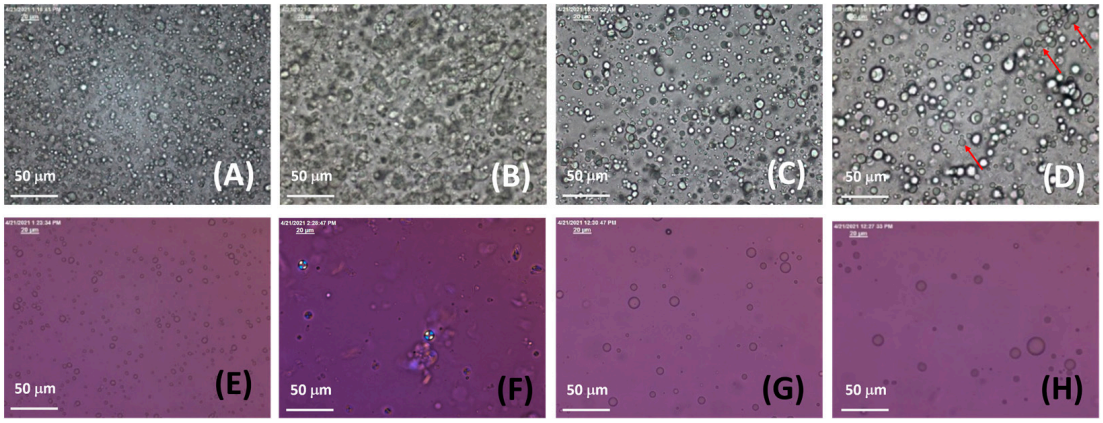


Figure 1. Images obtained from the optical observations in transmitted light (**A**–**D**) of concentrated samples and in cross-polarized light (**E**–**H**) of samples diluted with 5 mM SDS of emulgels containing 1% *w*/*w* Carbopol and 5% *w*/*w* (**A**,**E**) LLP (C1_LLP5 formulation), (**B**,**F**) CA (C1_CA5 formulation), (**C**,**G**) IPM (C1_IPM5 formulation) and (**D**,**H**) AO (C1_AO5 formulation). The red arrows in panel (**D**) indicate droplet coalescence.

The possible formation of onion-like lamellar structures in the CA-containing emulgels may be associated with the phase behavior and relatively high melting temperatures of Span 60 and cetyl alcohol. The optical features suggesting such an organization were observed only in the CA-containing formulations. This observation is consistent with the relatively high phase transition temperatures of both components: 52.9 °C for the transition from ordered to melted hydrocarbon chains in Span 60 [50–52] and 49.3 °C for the melting of cetyl alcohol [53]. Consequently, both components may contribute to the formation of ordered structures within the dispersed phase at room temperature. Similar spontaneous formation of onion-like structures from Span 60–CA mixtures in water is reported in [53]. Conversely, LLP and AO have melting points below 0 °C, forming liquid oil drops.

Quantitative analysis of the microscopy images showed that, for formulations containing 1% Carbopol and 5% oil phase, the mean droplet diameter (d_{32}) increased in the order LLP < IPM < AO, with values of 4.33, 6.38, and 10.56 µm, respectively (Table 2). The polydispersity index (PDI) followed the same trend, increasing from 1.12 for LLP to 1.19 for IPM and 1.24 for AO. Microscopic observations further revealed that the irregularly shaped dispersed particles in CA-containing formulations were considerably larger than the droplets observed in the other systems. Thus, the overall qualitative trend in dispersed-phase particle size was LLP < IPM < AO < CA. However, reliable quantitative size determination was not possible for the CA-containing formulations due to the irregular morphology of these particles.

Table 2. Droplet size characteristics of the investigated emulgel and bigel formulations: Sauter mean diameter (d_{32}), volume-weighted mean diameter (d_{43}), and polydispersity index (PDI = d_{43}/d_{32}).

Formulation Code	d_{32}, mm	d_{43}, mm	PDI (d_{43}/d_{32})
C1_LLP5	4.33	4.83	1.12
C1_LLP6	11.98	16.70	1.39
C1_LLP7.5	9.75	13.91	1.43
C1_CA5	-	-	-
C1_IPM5	6.38	7.56	1.19
C1_AO5	10.56	13.07	1.24
C0.5_LLP5	20.54	27.77	1.35
C0.5_LLP6	15.32	23.94	1.56
C0.5_LLP7,5	30.18	42.87	1.42
C0.5_CA5	-	-	-
C0.5_IPM5	7.29	9.09	1.25
C0.5_AO5	11.43	12.97	1.13
BG20	4.58	5.43	1.19
BG30	7.49	9.87	1.32

Interestingly, this trend was not maintained at the lower Carbopol concentration (0.5%). The corresponding d_{32} values were 20.54, 7.29, and 11.43 µm for LLP, IPM, and AO, respectively. Reducing the Carbopol concentration resulted in a pronounced increase in droplet size for LLP-based formulations, a smaller increase for IPM, and only a minor change for AO. These results indicate that the influence of Carbopol concentration on droplet size depends on the oil phase, highlighting the importance of both parameters in determining the microstructure of the investigated formulations.

Optical microscopy of the bigel samples, prepared by combining a sorbitan monostearate/almond oil oleogel with a Carbopol hydrogel, revealed closely packed dispersed droplets within the continuous matrix (Figure 2A). Upon dilution with 5 mM SDS, approximately spherical droplets of varying apparent sizes became more clearly distinguishable (Figure 2B). The oleogel droplets in the diluted BG20 sample (Figure 2B) exhibited a morphology similar to that observed in the diluted AO-containing emulgels (Figure 1H). However, quantitative analysis revealed that BG20 had smaller droplets than both AO-containing emulgels, despite its intermediate Carbopol concentration, while the polydispersity indices were comparable (Table 2). Since both formulations contain almond oil, differences in refractive index associated with the use of different oils do not directly affect this comparison. Nevertheless, differences in dispersed-phase composition and interfacial properties may influence optical contrast and apparent droplet boundaries.

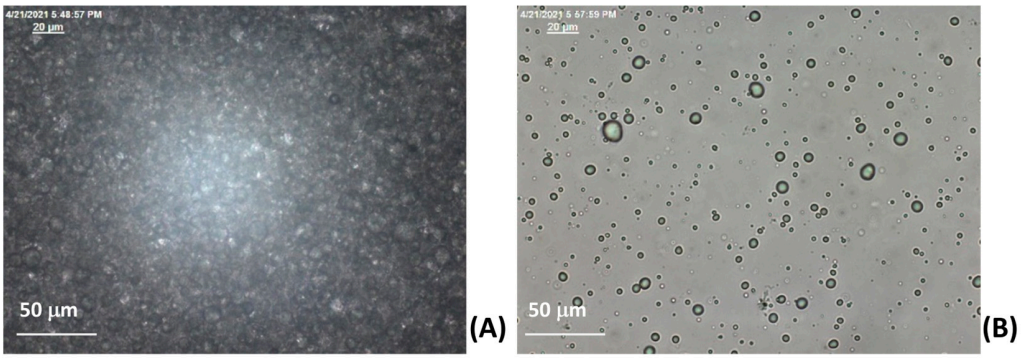


Figure 2. Images obtained from the optical observations in transmitted light of bigel BG20 (**A**) concentrated and (**B**) diluted with 5 mM SDS.

3.2. Rheological Properties of the Prepared Emulgels and Bigels

Four different rheological tests were performed with the studied emulgels and bigels aiming to obtain a robust rheological profile essential for optimizing formulation performance and end-use characteristics. The experiments included: (1) amplitude sweep tests to determine the linear viscoelastic region, establishing the limits within which the material maintains its structural integrity under strain; (2) frequency sweep tests performed within the linear viscoelastic region to explore the viscoelastic moduli as a function of oscillatory frequency, providing information on the gel-like or fluid-like nature of the systems; (3) steady shear tests to assess flow behavior and viscosity profiles under varying shear rates, revealing insights into the systems' pseudoplasticity and shear-thinning behavior; and (4) temperature ramp tests that were conducted to evaluate the thermal stability and transitions in rheological properties, simulating conditions relevant to storage and application.

3.2.1. Effect of the Oil Type in Emulgels

The effect of oil type in emulgels was studied at two different Carbopol concentrations: 0.5% *w*/*w* and 1% *w*/*w*. The obtained experimental results from rheological tests are shown in Figure 3 (1% *w*/*w* Carbopol) and Figure 4 (0.5% *w*/*w* Carbopol), and their statistical assessment in Tables S2 and S3.

As shown in Figure 3A, at the low deformation values, both the G′ and G″ moduli are not influenced by the increase in the applied strain, defining the so called "plateau-region" that represents the linear viscoelastic region. In this region, a well-visible predominance of the elastic modulus over the loss modulus was determined, indicating formation of a continuous gel structure. After a certain strain value, some destruction of the elastic structure of the emulgels occurs, resulting in a decrease in the elastic modulus, whereas the loss modulus started to increase, demonstrating that the formulations become more fluid.

Upon additional increase in the strain, a crossing of the moduli curves was determined, indicating that the samples start to flow. The obtained viscoelastic modulus curves were comparable to those reported for emulsions, xanthan gum-based gel systems, and Carbopol gels in previous studies [54–56]. The decrease in elasticity at high amplitude of deformation was associated with the arrangement of the system layers following the flux direction which caused better spreading of the emulgels upon dermal application. Such behavior is characteristic of structured polymeric emulgels and is consistent with the research of Dabbaghi et al., according to which the end of the linear viscoelastic range is associated with a critical shear stress that leads to the rupture of the three-dimensional gel network [57].

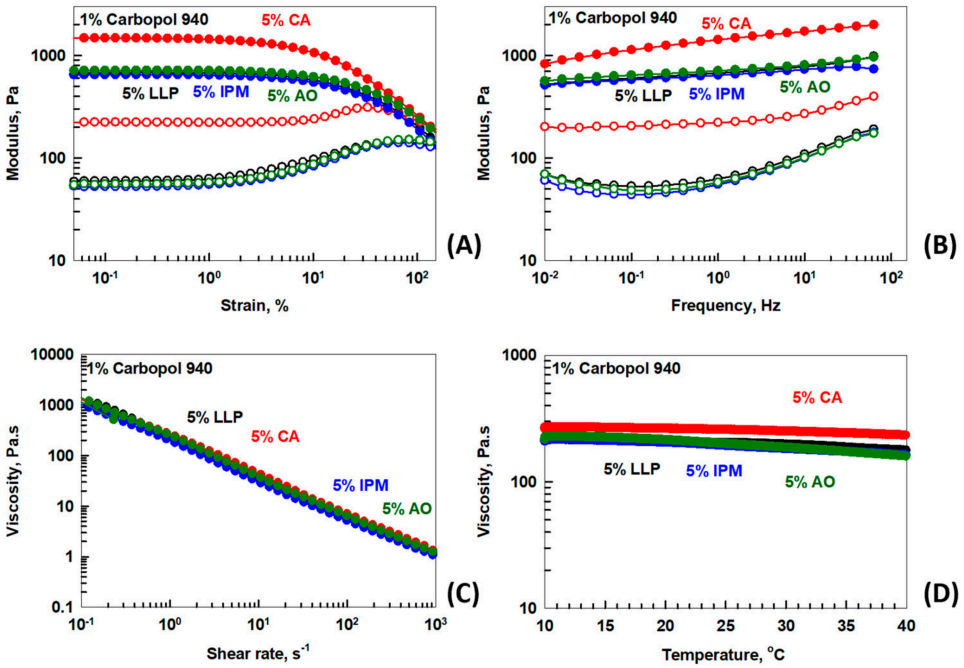


Figure 3. The rheological profile of the studied emulgels containing 1% *w*/*w* Carbopol and 5% *w*/*w* oil phase: LLP (black), CA (red), IPM (blue), or AO (green) as denoted in the graphs. Data are presented for the elastic, G′, (full symbols), and viscous, G″, (empty symbols), moduli as a function of (**A**) strain amplitude at a fixed frequency of deformation of 1 Hz and (**B**) frequency of oscillations at a fixed amplitude of deformation of 0.1%, as well as for the viscosity as a function of (**C**) shear rate and (**D**) temperature. The measurements presented in (**A**–**C**) were performed at 32 °C.

The observed behavior of the rheology curves was common for all studied formulations in this series, independent of the oil phase type (Figure 3A). The rheology response of the LLP, IPM and AO-containing emulgels largely overlapped. At the relatively low dispersed-phase volume fractions investigated in this study, differences in the viscosity of the individual liquid oils are not expected to substantially affect the overall rheological behavior of the emulgels. Instead, their rheological properties are expected to be predominantly governed by the continuous Carbopol-containing phase.

However, the CA-containing emulgel exhibited higher values of both G′ and G″ compared to the other formulations (Figure 3A). These higher moduli may be associated with the distinct microstructure of the CA-containing emulgel, characterized by the presence of birefringent dispersed particles observed under cross-polarized light (Figure 1F). Differences in the size, rigidity, and interactions of the dispersed particles with the Carbopol network may also contribute to the observed rheological behavior. The difference in the rheology of the CA-containing formulations compared to the other studied emulgels is even more significant in the case of the lower Carbopol concentration of 0.5% *w*/*w* (Figure 4A). In this case, no plateau region was determined even at the lower strain applied for the

CA-containing formulation and in the whole strain diapason, a decrease in the elastic modulus was determined. Concerning the viscous modulus, we observed significantly higher values for it, which were even higher than these of the elastic moduli of the other studied systems at the lower and higher values of the deformation. There is a region, however, in which a slight minimum is observed in this curve, which then crosses that of the elastic modulus of the sample (Figure 4A). Such a significant difference in the rheology curves that this CA-containing sample exhibited could probably be due to insufficient homogeneity of the sample. Nevertheless, the CA-containing formulation maintained higher viscoelastic moduli than the other emulgels, consistent with the behavior observed at 1% *w*/*w* Carbopol. This further suggests that differences in the organization of the dispersed phase may contribute to the rheological behavior of the CA-containing systems.

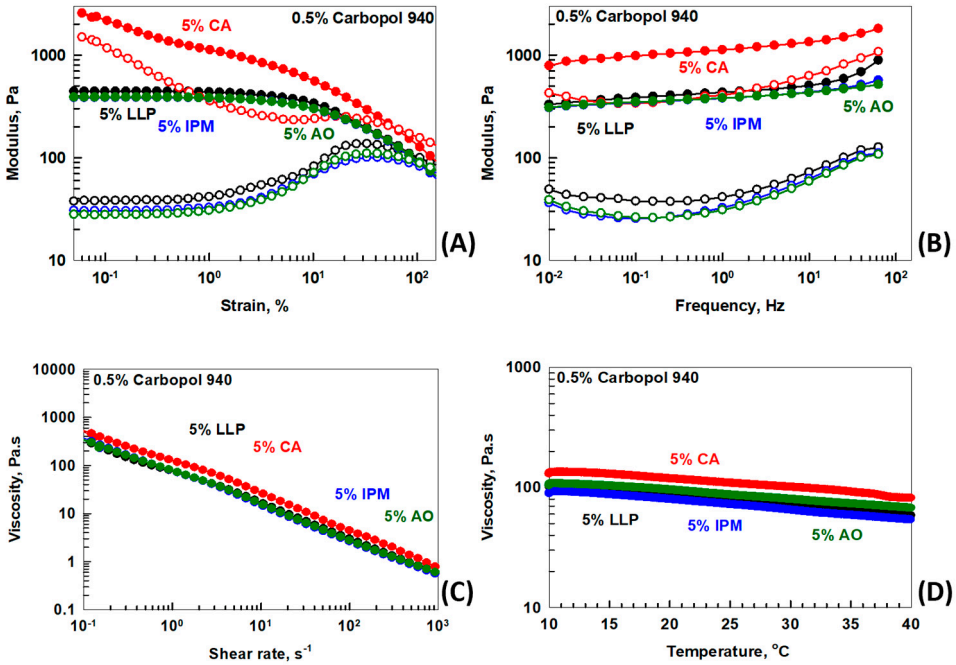


Figure 4. The rheological profile of the studied emulgels containing 0.5% *w*/*w* Carbopol and 5% *w*/*w* oil phase: LLP (black), CA (red), IPM (blue) or AO (green) as denoted in the graphs. Data are presented for the elastic, G′, (full symbols) and viscous, G″, (empty symbols) moduli as a function of (**A**) strain amplitude at a fixed frequency of deformation of 1 Hz and (**B**) frequency of oscillations at a fixed amplitude of deformation of 0.1%, as well as for the viscosity as a function of (**C**) shear rate and (**D**) temperature. The measurements presented in (**A**–**C**) were performed at 32 °C.

The particular G′ and G″ values of the LLP, IPM, and AO-containing emulgels were lower in the case of lower Carbopol concentration (Figure 4A), but the rheology curves of the systems containing these oil phases overlap independently of the oil phase type, indicating similarity in the viscoelastic properties.

The higher values of the moduli in the case of 1% *w*/*w* Carbopol revealed that an increase in the concentration of the gelling agent causes greater elasticity of the tested models. This is related to the higher amount of polymer that enables the interaction and interweaving of the polymer chains, hence resulting in the formation of a strong polymer network. The obtained results confirmed the conclusions of other authors who have investigated the viscoelastic properties of Carbopol gels with various concentrations [58]. Since it has been established that the gelling agent has a substantial impact on the emulgel rheological properties [59], we could suppose that the rheological characteristics of the studied formulations in the current work would correspond to the rheological properties of Carbopol gels, as it is the gelling agent in the samples.

Based on these results obtained from the amplitude sweep experiments, we determined the yield stress values for the studied systems, which were extracted by analyzing plots of the calculated elastic stress, τelastic, (τelastic = G′γ0) versus strain amplitude, γ0, [60]. Within the linear viscoelastic region, $\tau_{elastic}$ increases linearly with increasing strain amplitude until the material reaches a critical shear stress (corresponding to the yield stress) defined as the strain at which τelastic attains its maximum value (Figure S2 in SI). The dependence of yield stress on the oil phase composition is presented in Figure S3A (SI) for both Carbopol concentrations. The results clearly demonstrate that the yield stress is significantly affected by the polymer content, with samples containing higher levels of Carbopol exhibiting markedly greater values. The rheological behavior also reflects differences in the microstructure of the investigated formulations. In particular, the CA-containing emulgels, characterized by birefringent dispersed particles, exhibited the highest yield stress at both Carbopol concentrations, suggesting that the distinct organization of their dispersed phase may contribute to their greater resistance to deformation. Conversely, formulations containing liquid paraffin (LLP) or isopropyl myristate (IPM) showed the lowest yield stress, while those with almond oil (AO) exhibited intermediate values at higher Carbopol levels. The elevated yield stress observed for AO-based emulgels relative to LLP- and IPM-containing systems at 1% Carbopol 940 may be associated with differences in the interfacial interactions and chemical composition of the oils. Almond oil consists predominantly of unsaturated triglycerides and contains minor amphiphilic constituents, which may contribute to differences in polarity and interfacial behavior compared to less polar oils, such as liquid paraffin. These characteristics could potentially favor interactions with the hydrophilic domains of the Carbopol network and with the surfactant-stabilized oil–water interface, particularly at higher polymer concentrations. Such interactions may contribute to a more cohesive gel structure with greater resistance to deformation, resulting in higher yield stress values. In contrast, weaker interactions between the dispersed phase and the polymer network in LLP- and IPM-containing formulations could contribute to their lower yield stress. The differences between AO- and LLP/IPM-based formulations become less pronounced at lower Carbopol concentrations, possibly due to a reduced contribution of these interactions. However, this interpretation remains hypothetical, and its experimental verification would require further investigation of the interactions between the oil components, surfactants, and Carbopol network, which is beyond the scope of the present study.

The experimental data from frequency sweep experiments of the emulgels are shown in Figures 3B and 4B. In all of the studied formulations, G′ consistently exceeded G″ across the tested frequency range, showing again that the emulgels possess a mainly elastic character. The obtained rheology curves in our frequency sweep experiments for LLP, IPM and AO-containing samples again overlap as in the case of the amplitude sweep tests, whereas the data for the CA-containing emulgel were well above those of the other formulations (Figures 3 and 4). This difference may be associated with its distinct microstructure, particularly the presence of birefringent dispersed particles observed under cross-polarized light (Figure 1F).

The flow curves of the studied emulgels, shown in Figures 3C and 4C, illustrate how the viscosity of the formulations with different oil phases changes in response to different shear rates at a constant temperature of 32 °C. All samples displayed a typical non-Newtonian, shear-thinning behavior—an important feature for topical products, as it allows them to become less viscous during application [61]. This is well seen from the results shown in Figures 3C and 4C, where the rheology curves for the viscosity of the studied emulgels are shifted to higher values for the higher gelling agent concentration, as expected. Concerning the effect of the studied oil phases on the viscosity of the respective formulations, one can

see that for the samples containing 1% *w*/*w* Carbopol it is negligible, and all the rheology curves overlap (Figure 3C). In the case of 0.5% *w*/*w* gelling agent, the LLP, IPM, and AO samples show even closer values of the viscosity as a function of the shear rate, and their rheology curves practically coincide. The presence of CA, however, affects the emulgel viscosity at the lower Carbopol concentration, with the corresponding flow curve showing a slight shift towards higher viscosity values. This behavior may be associated with the distinct microstructure of the CA-containing formulation.

All flow curves were fitted using the Herschel–Bulkley model, and the obtained fitting parameters are presented in Table S1. The Herschel–Bulkley model provided an excellent fit to the experimental data, with coefficients of determination (R^2) exceeding 0.999 for most formulations. The only exception was formulation C0.5_CA5, for which a slightly lower R^2 value of approximately 0.98 was obtained. Nevertheless, this value still indicates very good agreement between the experimental data and the model predictions.

The fitting results clearly demonstrate that formulations containing CA exhibit substantially different rheological behavior compared to the corresponding formulations prepared with the other oils at the same Carbopol concentration. In addition, as expected, both the yield stress and the consistency index increased with increasing Carbopol concentration, confirming the dominant role of the polymer network in determining the flow properties of the systems. These findings are consistent with the conclusions of a review paper that analyzes the combined effects of concentration and pH on the Herschel–Bulkley parameters for Carbopol 934, 940, 980, and Ultrez. The author explicitly states that both the yield stress and the consistency index increase monotonically with rising concentration, as the microgel particles become more densely packed and more firmly interlocked with one another [62]. Our results are also consistent with an earlier study, which directly demonstrates that increasing the concentration of Carbopol significantly raises the yield stress, viscosity, and consistency index, confirming the dominant role of the dense three-dimensional network of swollen polymer chains [63].

For all formulations, the flow behavior index (n) ranged between approximately 0.3 and 0.4, indicating pronounced non-Newtonian behavior and a highly shear-thinning character. Such values are typical of structured semisolid systems and suggest that the formulations can be easily spread under shear while maintaining sufficient consistency at rest.

In order to assess the thermal stability of emulgels, we performed viscosity measurements of the studied emulgels as a function of temperature in the range between 10 °C and 40 °C with a rate of 5 °C/min at a fixed shear rate of 1 s^{-1}; see Figures 3D and 4D. No abrupt changes in viscosity were observed within the investigated temperature range, suggesting the absence of major thermally induced structural transitions. This is consistent with the melting temperatures of Span 60 and CA being above 40 °C. The CA-containing formulations exhibited higher viscosity than the other emulgels throughout the investigated temperature range (Figures 3D and 4D), which may be associated with their distinct dispersed-phase microstructure.

It should be noted that these measurements were performed within the temperature range of 10–40 °C to assess the rheological behavior of the formulations under application-relevant conditions rather than to identify phase transitions. Although no abrupt viscosity changes were observed within this range, structural transitions at higher temperatures cannot be excluded. Further investigations, including oscillatory temperature sweeps over an extended temperature range and thermal or structural characterization, would be required to identify possible phase transitions in the CA-containing systems.

Concerning the effect of the Carbopol concentration, again the emulgels with 1% Carbopol showed higher viscosity in the whole temperature range compared to that of the 0.5% Carbopol-containing samples. The viscosity of the formulations with the higher

Carbopol level decreased by 11–26% compared to the 35–40% decrease in the case of the systems with lower Carbopol concentration upon temperature increase. This result is related to a denser polymer network formed at higher Carbopol concentration, which has more crossed bonds between the polymer chains in the polymer structure. This increased number of crossed bonds reduces the thermal mobility of the individual polymer chains, thus causing less significant changes in viscosity and, hence, increased stability.

3.2.2. Effect of the Oil Phase Concentration in Emulgels

To further explore formulation parameters, LLP-based emulgels were prepared with different oil content of 5, 6, and 7.5% *w*/*w* at two Carbopol levels (0.5 and 1% *w*/*w*). The obtained results are shown in Figure 5 and their statistical assessment in Table S4. One sees that the oil concentration has no significant impact on the rheological properties of the formed emulgels, showing that the presence of oil drops in the hydrogel does not significantly reinforce the gel network formed from Carbopol. All tests indicate that the gelling agent concentration is significantly more critical for the rheological properties of formed emulgels. This trend is also reflected in the determined yield stress, which does not change significantly within the studied LLP concentration range (Figure S3B in SI).

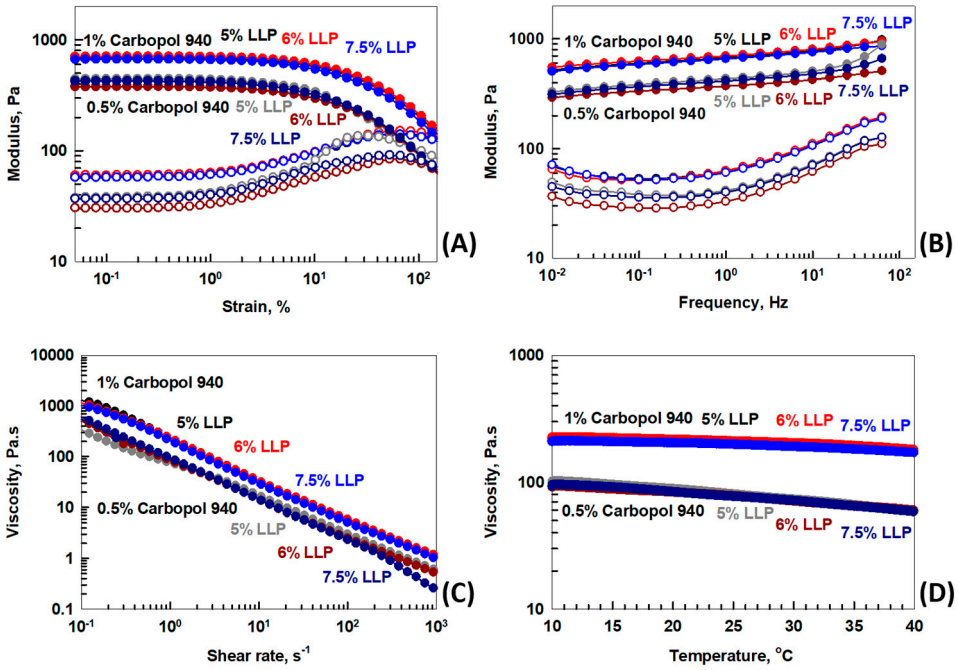


Figure 5. The rheological profile of the studied emulgels containing 0.5 or 1% *w*/*w* Carbopol and different concentrations of LLP as denoted in the graphs. Data are presented for the elastic, G′, (full symbols) and viscous, G″, (empty symbols) moduli as a function of (**A**) strain amplitude at fixed frequency of deformation of 1 Hz and (**B**) frequency of oscillations at fixed amplitude of deformation of 0.1%, as well as for the viscosity as a function of (**C**) shear rate and (**D**) temperature. The measurements presented in (**A**–**C**) are performed at 32 °C.

The Herschel–Bulkley fitting results (see Table S1) support that the dominant factor governing the rheological behavior of the investigated formulations is the Carbopol concentration. The effect of oil concentration appears to be negligible and, for most systems, remains within the experimental standard deviation. This observation is consistent with the fact that the continuous Carbopol network primarily determines the flow properties of the formulations, while variations in oil content have only a minor influence on the fitted rheological parameters.

Although the moduli decreased substantially at lower Carbopol concentrations, no systematic dependence on oil concentration was observed (Figure 5B). The minor variations in the moduli, particularly at high frequencies, did not follow a consistent trend with increasing oil content. These observations further support the conclusion that the viscoelastic properties of the investigated emulgels are predominantly governed by the Carbopol concentration rather than by variations in the oil content within the studied range.

3.2.3. Effect of the Oleogel Concentration in Bigels

To assess the influence of oil structuring on gel properties, almond oil was incorporated either as liquid oil (emulgel) or as an oleogel dispersed within Carbopol hydrogel (bigels). Additionally, the effect of the oleogel concentration was also studied as a comparison between the pure hydrogel (0% oleogel), BG20 (20% oleogel), BG30 (30% oleogel), and the pure oleogel (100% oleogel).

Amplitude sweep results (Figure 6A) revealed clear structural hierarchies. The oleogel exhibited the weakest network, reaching flow at low strain. Hydrogel and emulgel showed similar plateau moduli, while both bigel formulations demonstrated enhanced elasticity, with BG30 displaying the highest G′. The storage modulus (G′) of BG20 is approximately 20% higher than that of the corresponding hydrogel and about 13 times higher than that of the oleogel. An even stronger effect is observed for BG30, whose storage modulus is approximately 80% higher than that of the hydrogel and about 20 times higher than that of the oleogel. Similar, and even more pronounced, trends are observed for the loss modulus (G″). These results indicate that the mechanical properties of the bigels cannot be explained as a simple additive contribution of the individual gel phases. Instead, the higher moduli of the bigels compared to both individual gel phases suggest synergistic mechanical reinforcement upon combining the oleogel and hydrogel components, although the specific interactions responsible for this enhancement remain to be established. The difference between BG20 and BG30 is particularly notable, indicating that increasing the oleogel content from 20% to 30% resulted in higher elastic moduli and greater mechanical reinforcement of the bigel structure. Furthermore, in our previous study [45], increasing the oleogel content to 40% resulted in structural instability and disruption of the bigel structure. Taken together, these findings suggest that an optimal oleogel content exists within the investigated formulation system, with 30% providing the most favorable balance between mechanical reinforcement and structural stability among the compositions studied. The viscous moduli, G″ followed the same order: oleogel << hydrogel ≈ emulgel < BG20 < BG30 (Figure 6A). It is particularly noteworthy that in the plateau region the elastic modulus of the oleogel is similar in value to that of the viscous modulus of the emulgel, emphasizing the weak structural capacity of the oleogel. A balance between structure and fluidity is reflected by the moderate G″ values measured for the studied hydrogel and emulgel. The bigels, however, particularly the BG30 formulation, demonstrated enhanced viscous behavior. Frequency sweeps (Figure 6B) supported these findings: G′ exceeded G″ across the measured range for all samples except the oleogel, which showed a crossover at higher frequencies. Both BG20 and BG30 exhibited higher moduli than the emulgel or hydrogel alone, with BG30 again proving most elastic and showing synergistic reinforcement in the mixed gel systems.

It is important to note that the Carbopol concentration was not identical in all formulations. The emulgel contained 1.0 wt% Carbopol, whereas the Carbopol concentrations in BG20 and BG30 were 0.8 wt% and 0.7 wt%, respectively. This reduction resulted from the dilution of the hydrogel phase during blending with the oleogel. Therefore, the observed enhancement in the rheological properties of the bigels cannot be attributed to a higher Carbopol concentration but rather to the synergistic interactions between the oleogel and hydrogel networks.

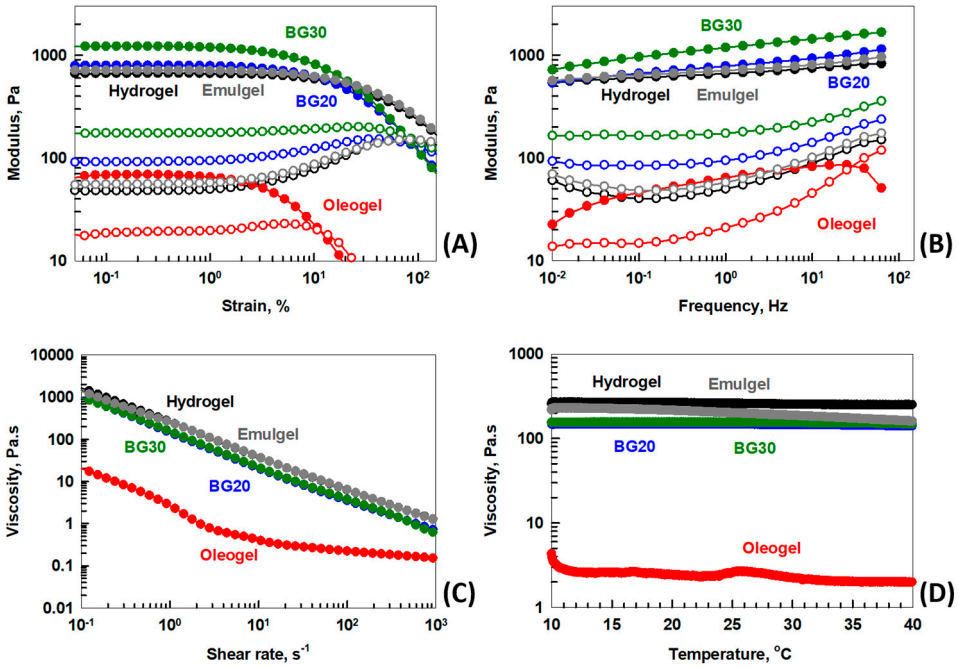


Figure 6. Comparison between the rheological profile of the studied bigels containing different concentrations of oleogel (0%, 20%, 30% and 100%) and the respective emulgel. Data are presented for the elastic, G′, (full symbols) and viscous, G″, (empty symbols) moduli as a function of (**A**) strain amplitude at fixed frequency of deformation of 1 Hz and (**B**) frequency of oscillations at fixed amplitude of deformation of 0.1%, as well as for the viscosity as a function of (**C**) shear rate and (**D**) temperature. The measurements presented in (**A**–**C**) are performed at 32 °C.

The oil phase incorporation manner does not influence the shear-thinning behavior of the samples (Figure 6C). Such pseudoplastic flow of bigels is commonly reported in the literature as observed for instance with sesame oil/Span® 60/Carbopol®940 bigels [18]. The hydrogel and emulgel were the most viscous, whereas the oleogel was the least, as the difference between these systems was determined to be of around two orders of magnitude (Figure 6C). The bigels exhibited intermediate values close to one another. Incorporation of oleogel reduced viscosity relative to the hydrogel but did not change the flow profile. A similar comparison between the viscosity of the hydrogel, oleogel and the different blends between them is reported in the literature [19].

The Herschel–Bulkley fitting results (see Table S1) further confirm that the rheological parameters of the hydrogel are very similar to those of the corresponding emulgel. In contrast, the oleogel exhibited the lowest values of both yield stress and consistency index. Moreover, the flow behavior index of the oleogel was approximately 0.8, indicating a markedly different flow behavior compared to all other formulations investigated in this study.

The bigels displayed intermediate rheological characteristics between those of the hydrogel and the oleogel. Among them, BG30 exhibited higher yield stress and consistency index values than BG20, indicating a stronger and more resistant network structure.

Temperature ramp tests demonstrated that the emulgel and bigel formulations maintained relatively stable rheological behavior within the investigated temperature range of 10–40 °C, whereas the oleogel exhibited more pronounced temperature-dependent changes (Figure 6D). Since the oleogel consists of almond oil and Span 60, these changes may be associated with temperature-dependent rearrangements of the Span 60-based structuring network. However, confirming whether crystallization or other thermal transitions contribute to the observed behavior would require additional investigations, including DSC

measurements and oscillatory temperature sweeps over an extended temperature range, to establish possible relationships between thermal transitions and changes in the viscoelastic properties of the oleogel and bigel formulations.

All these rheological results, including the statistical analysis (Table S5), demonstrate the superior mechanical performance of BG30 compared to BG20, despite its lower hydrogel content. Furthermore, in our previous study [45], increasing the oleogel content to 40% resulted in structural instability and disruption of the bigel structure. Taken together, these findings suggest that an optimal balance between the hydrogel and oleogel phases may exist, rather than simply maximizing the hydrogel fraction, with BG30 exhibiting the most favorable mechanical properties among the investigated formulations. The observed increase in elasticity with increasing oleogel fraction may be explained by a mechanism analogous to that commonly observed in concentrated emulsions, where increasing the dispersed-phase volume fraction enhances the mechanical resistance of the system. Although the oleogel fractions investigated here are considerably below the close-packing limit typically associated with concentrated emulsions, a similar mechanism may contribute to the rheological behavior of the bigels. In these systems, the dispersed droplets are embedded within a continuous hydrogel network, which restricts their movement and rearrangement under deformation. Increasing the oleogel fraction may further enhance these constraints, resulting in greater resistance to deformation and, consequently, a higher elastic modulus. Thus, the observed reinforcement does not necessarily require close packing of the dispersed droplets but may arise from the combined contribution of the dispersed oleogel phase and the surrounding polymer network. The emulgel also offers favorable mechanical properties, combining moderate elasticity and viscosity with good spreadability, making it suitable for topical applications. In contrast, the oleogel, though structurally weakest on its own, can significantly enhance the mechanical profile of multiphase gel-based dispersion systems like bigels when appropriately integrated. This highlights the importance of phase interactions and composition balance in designing gel-based delivery systems for pharmaceutical and cosmetic applications. The conclusions drawn are consistent with actual research in the field of pharmaceutical and cosmetic formulations. For instance, one study describes how, upon exceeding the limit of dense packing (ϕ approx 0.64–0.74), the droplets become "jammed", losing their ability to move freely relative to one another, undergoing deformation, and causing a sharp increase in the elastic modulus (G′) and the mechanical stability of the system [64]. Another study investigates the influence of hydrogel/oleogel ratios (e.g., 67:33, 83:17), with the authors demonstrating that altering the oleogel fraction changes the mechanical response (viscosity, elasticity, hardness) and that there is a strictly critical and optimal ratio for stability without phase separation [65].

3.3. Long-Term Stability of the Studied Emulgels and Bigels

Apart from the temperature ramp rheology experiments, a long-time stability test was performed for all the studied samples as assessed in accordance with International Council for Harmonisation guidelines. For this experiment, the emulgels and bigels were packed in tightly closed plastic containers and stored at 30 ± 2 °C/65 ± 5% RH. After 12 months, the samples were evaluated for physical appearance. All samples were determined to be stable for 12 months without any change in their visual appearance.

Conventional accelerated stability testing involves storage under elevated temperature and humidity conditions, typically 40 ± 2 °C/75 ± 5% RH for six months, according to ICH Q1A(R2). In contrast, temperature-ramp rheology provides a rapid assessment of the rheological response of formulations to continuously changing temperature. Similar temperature-dependent rheological approaches have been employed to predict temperature-induced instability in hydrogel-based materials [66].

The agreement between the temperature ramp rheological results and the long-term visual stability observations provides two independent lines of evidence supporting the physical stability of the investigated formulations. These findings also suggest that temperature ramp rheology may be a useful complementary approach for the preliminary assessment of formulation stability.

3.4. Correlation Between Rheology, Drug Release and Spreadability

Rheological properties of dermal formulations are intrinsically linked to their stability, sensory attributes, and patient compliance. Importantly, rheology also governs drug delivery performance by influencing the release profile [1–3].

Rheological properties play an important role in determining the functional performance of semi-solid formulations. Viscosity and viscoelasticity reflect the resistance of the formulation to flow and deformation and may influence drug release by affecting the structure of the vehicle and the mobility of its components [67,68]. Yield stress and shear-thinning behavior are particularly relevant to spreadability, as they determine the resistance to flow during application [69]. A sufficiently high yield stress helps maintain the formulation at the application site, whereas excessive resistance to flow may hinder spreading. Viscoelastic properties may also influence the structural integrity and retention of the formulation after application [70,71]. Consequently, an appropriate balance between viscosity, elasticity, and flow behavior is important for achieving desirable application characteristics and patient acceptability. However, drug release also depends on other factors, including drug solubility, thermodynamic activity, and interactions with the formulation components [72]. In this study, we extend the structural and rheological characterization of the investigated systems by establishing correlations with drug release and spreadability. The drug release and spreadability data were previously reported in our earlier work [46], which formed part of a broader research project focused on the development and characterization of semi-solid dosage forms and the evaluation of their functional performance. The novelty of the present study lies in combining these previously published data with the detailed rheological characterization performed here to provide a new correlation analysis exploring the relationships between microstructure, viscosity, yield stress, viscoelasticity, drug release, and spreadability. Accordingly, correlation plots were constructed between key rheological parameters (viscosity, yield stress, and G′), spreadability, and drug release performance (cumulative release and time required for 50% release, t_{50}%), as shown in Figures 7 and S4 in the SI.

Importantly, the rheological characterization, drug release studies, and spreadability measurements were all conducted using the same materials, formulations, and preparation batches, minimizing potential effects of batch-to-batch variability on the comparisons presented here.

The analysis revealed an apparent viscosity threshold of approximately 150 Pa·s, above which markedly reduced drug release was observed (Figures 7A and S4A in the SI). Below this value, cumulative release increased substantially, highlighting the importance of viscosity for drug release within the investigated formulations. Although the relationship was nonlinear, the observed trend illustrates the interplay between rheological properties, structural characteristics, and drug release performance.

Yield stress displayed a comparable pattern: samples exceeding a critical yield stress exhibited minimal release after 150 min, whereas those below the threshold demonstrated significantly higher release (Figure 7B). Correlation of elastic modulus with release kinetics showed that t_{50}% remained relatively constant within a plateau region before rising steeply once G′ surpassed a critical value (Figure 7C). However, no consistent relation was observed between G′ and long-term drug release (Figure S4B–D in SI).

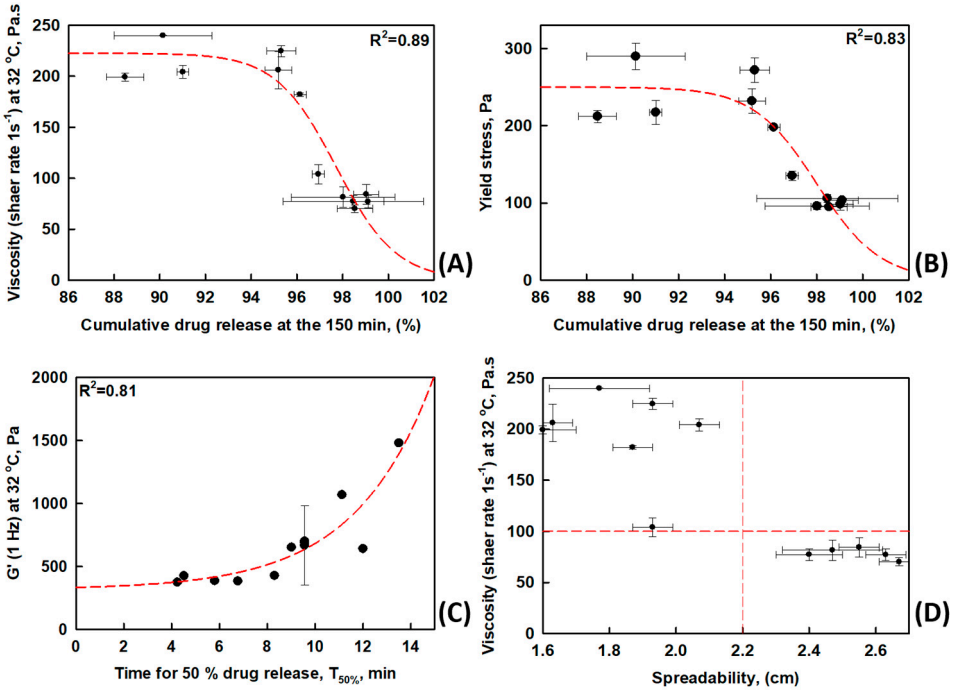


Figure 7. Correlations between different rheology parameters and formulations' properties, as constructed for the Carbopol-containing emulgels. Data are presented for the relation between (**A**) the viscosity as measured at 32 °C and the cumulative drug release at 150 min; (**B**) the yield stress of the samples and the cumulative drug release at 150 min; (**C**) the elastic modulus and the time for 50% drug release, $t_{50\%}$; and (**D**) the viscosity as measured at 32 °C and the spreadability of the respective formulations. The red dashed line represents the fit to the experimental data.

In parallel, application-related attributes were assessed. Spreadability, an important factor influencing patient acceptability, showed a clear inverse relationship with viscosity (Figures 7D and S4E–G in the SI): high-viscosity formulations exhibited lower spreadability, whereas low-viscosity systems were more easily distributed. Importantly, formulations combining lower viscosity with higher spreadability also exhibited enhanced in vitro drug release, highlighting the close relationship between rheological properties and the functional performance of semi-solid formulations.

The obtained results demonstrate the important role of viscosity, yield stress, and viscoelastic properties in controlling drug release and spreadability. Lower viscosity and yield stress generally favor faster in vitro drug release and improved spreadability, whereas excessively low viscosity may compromise structural integrity and long-term stability. Thus, formulation design requires careful adjustment of rheological properties to achieve an optimal balance between stability, spreadability, and drug release performance. Nevertheless, in vitro drug release measurements do not account for the barrier properties of the skin or the complexity of drug transport under physiological conditions. Therefore, the observed relationships cannot be directly extrapolated to skin permeation, bioavailability, or therapeutic efficacy. Further skin permeation and in vivo studies are required to establish the physiological relevance of these findings.

4. Conclusions

This study provides a microstructural and rheological characterization of emulgels and bigels formulated with different oil phases and Carbopol concentrations, with additional insights into their drug release and spreadability. Microscopic observations revealed dispersed droplets embedded within the continuous hydrogel matrix of the investigated

emulgels and bigels, with differences in droplet morphology and size depending on the formulation composition.

The type of oil was shown to be an important factor influencing the morphology and size distribution of the dispersed particles. In particular, cetyl alcohol-containing formulations exhibited larger, irregular birefringent particles with Maltese cross-like patterns, suggesting possible internal structural organization that may contribute to their distinct rheological behavior.

Rheological testing revealed that all systems exhibited shear-thinning, pseudoplastic flow and gel-like properties ($G' > G''$ across relevant frequency ranges), favorable for dermal applications. Carbopol concentration emerged as the dominant parameter determining elasticity, viscosity, and temperature resistance, while oil type and structuring played a modulatory role, particularly through the formation of ordered aggregates in cetyl alcohol systems. Bigels demonstrated enhanced elasticity compared with the corresponding emulgels, particularly at higher oleogel fractions, while maintaining relatively stable rheological behavior within the investigated temperature range (10–40 °C). The higher elastic moduli of the bigels, despite their lower Carbopol concentrations, suggest a possible synergistic mechanical reinforcement arising from the combination of the hydrogel and oleogel phases.

Correlation analysis revealed relationships between the rheological parameters (viscosity, yield stress, and elastic modulus) and the functional properties (drug release and spreadability) of the investigated formulations. Formulations with higher viscosity exhibited reduced release and poor spreadability, whereas systems with moderate viscosity provided a favorable balance between structural integrity, user acceptability, and release kinetics. When correlating rheological parameters with drug release, certain limitations must be taken into account, such as the specific nature of the skin barrier, thermodynamic activity, and the influence of excipients within the formulation. Rheological measurements are conducted in vitro under controlled temperature and shear conditions; however, they do not account for in vivo factors such as skin temperature and hydration, the presence of sebum and sweat, mechanical friction (which alters the structure of non-Newtonian fluids upon application), and microcirculation (the clearance of the drug from the dermis).

Hence, the current study demonstrates that rational selection of the oil phase, its structuring, and the gelling agent concentration allow fine-tuning of the structural, rheological, and functional properties of emulgels and bigels. The results emphasize the relevance of phase structuring and network reinforcement strategies for developing dermal formulations with enhanced stability, spreadability, and drug delivery performance, making them suitable candidates for topical therapeutic and cosmetic applications.

Supplementary Materials: The following supporting information can be downloaded at https://www.mdpi.com/article/10.3390/macromol6040107/s1: Figure S1. Images obtained from the optical observations in cross-polarized of emulgels containing CA; Table S1: Parameters of the Herschel–Bulkley model obtained from fitting the experimental flow curves; Table S2: *p*-values obtained from Student's *t*-test for the data presented in Figure 3; Table S3: *p*-values obtained from Student's *t*-test for the data presented in Figure 4; Table S4: *p*-values obtained from Student's *t*-test for the data presented in Figure 5; Table S5: *p*-values obtained from Student's *t*-test for the data presented in Figure 6; Figure S2: Elastic stress as a function of the strain for a representative emulgel sample; Figure S3: Yield stress for the investigated emulgel samples; Figure S4: Correlations between different rheology parameters and samples properties for the emulgels.

Author Contributions: Conceptualization, S.T.; methodology, S.T.-G. and S.T.; formal analysis, S.T.-G., P.P., Y.G. and N.P.-B.; investigation, S.T.-G., P.P. and Y.G.; data curation, S.T.-G.; writing—original draft preparation, S.T.-G., P.P. and N.P.-B.; writing—review and editing, Y.G., M.K. and S.T.; visualization, S.T.-G.; supervision, M.K. and S.T.; funding acquisition, Y.G., M.K. and S.T. All authors have read and agreed to the published version of the manuscript.

Funding: The support of the Centre of Competence "Sustainable Utilization of Bio-resources and Waste of Medicinal and Aromatic Plants for Innovative Bioactive Products" (BIORESOURCES BG), project BG16RFPR002-1.014-0001, funded by the Program "Research, Innovation and Digitization for Smart Transformation" 2021–2027, co-funded by the EU, is greatly acknowledged.

Institutional Review Board Statement: Not applicable.

Data Availability Statement: The raw data supporting the conclusions of this article will be made available by the authors upon request.

Acknowledgments: We would like to express our gratitude to the program "Research, Innovation and Digitalisation for Smart Transformation" 2021–2027, funded by the European Union, Project BG16RFPR002-1.014-0007 "Center for Competence "PERIMED-2" for supporting this article.

Conflicts of Interest: The authors declare no conflicts of interest.

Abbreviations

The following abbreviations are used in this manuscript:

LLP	Light liquid paraffin
CA	Cetyl alcohol
IPM	Isopropyl myristate
AO	Almond oil
TEA	Triethanolamine
SDS	Sodium dodecyl sulfate
PG	Propylene glycol

References

1. Kumar, I.; Kushwaha, S. Emulgels: Revolutionizing Topical and Transdermal Drug Delivery. *Int. J. Pharm. Sci.* **2025**, *3*, 2840–2850. [CrossRef]
2. Almeida, I.F.; Fernandes, A.R.; Fernandes, L.; Pena Ferreira, M.R.; Costa, P.C.; Bahia, M.F. Moisturizing Effect of Oleogel/Hydrogel Mixtures. *Pharm. Dev. Technol.* **2008**, *13*, 487–494. [CrossRef]
3. Martín-Illana, A.; Notario-Pérez, F.; Cazorla-Luna, R.; Ruiz-Caro, R.; Bonferoni, M.C.; Tamayo, A.; Veiga, M.D. Bigels as drug delivery systems: From their components to their applications. *Drug Discov. Today* **2022**, *27*, 1008–1026. [CrossRef]
4. Jagdale, S.C.; Kothekar, P.V. Development of Emulgel Delivery of Mupirocin for Treatment of Skin Infection. *Recent Pat. Antiinfect. Drug Discov.* **2020**, *15*, 137–156. [CrossRef]
5. Burki, I.K.; Khan, M.K.; Khan, B.A.; Uzair, B.; Braga, V.A.; Jamil, Q.A. Formulation Development, Characterization, and Evaluation of a Novel Dexibuprofen-Capsaicin Skin Emulgel with Improved In Vivo Anti-inflammatory and Analgesic Effects. *AAPS PharmSciTech* **2020**, *21*, 211. [CrossRef]
6. Soni, K.; Gour, V.; Agrawal, P.; Haider, T.; Kanwar, I.L.; Bakshi, A.; Soni, V. Carbopol-olive oil-based bigel drug delivery system of doxycycline hyclate for the treatment of acne. *Drug Dev. Ind. Pharm.* **2021**, *47*, 954–962. [CrossRef]
7. Srivastava, N.; Patel, D.K.; Rai, V.K.; Pal, A.; Yadav, N.P. Development of emulgel formulation for vaginal candidiasis: Pharmaceutical characterization, in vitro and in vivo evaluation. *J. Drug Deliv. Sci. Technol.* **2018**, *48*, 490–498. [CrossRef]
8. Khan, B.A.; Ullah, S.; Khan, M.K.; Alshahrani, S.M.; Braga, V.A. Formulation and evaluation of *Ocimum basilicum*-based emulgel for wound healing using animal model. *Saudi Pharm. J.* **2020**, *28*, 1842–1850. [CrossRef]
9. Zhu, Q.; Gao, J.; Han, L.; Han, K.; Wei, W.; Wu, T.; Li, J.; Zhang, M. Development and characterization of novel bigels based on monoglyceride-beeswax oleogel and high acyl gellan gum hydrogel for lycopene delivery. *Food Chem.* **2021**, *365*, 130419. [CrossRef]
10. Bollom, M.A.; Clark, S.; Acevedo, N.C. Edible lecithin, stearic acid, and whey protein bigels enhance survival of probiotics during in vitro digestion. *Food Biosci.* **2021**, *39*, 100813. [CrossRef]
11. Zhuang, X.; Clark, S.; Acevedo, N. Bigels—Oleocolloid matrices—As probiotic protective systems in yogurt. *J. Food Sci.* **2021**, *86*, 4892–4900. [CrossRef]
12. Ghinea, C.; Leahu, A. Oleogels, Bigels, and Emulgels: Fabrication, Application and Research Trends. *Gels* **2025**, *11*, 816. [CrossRef]
13. Dangi, M.; Setya, S.; Talegaonkar, S. Bigels: A comprehensive review of properties, preparation techniques, applications in pharmaceuticals, food, cosmetic products, and emerging patents. *J. Dispers. Sci. Technol.* **2026**, *47*, 2463–2493. [CrossRef]
14. Juchniewicz, S.; Harasym, J. Oxidation Mechanism in Bigels and Emulgels—Challenges and Solutions. *Molecules* **2026**, *31*, 970. [CrossRef]

15. Ojha, S.; Yadav, J. Recent Advances in Emulgel Technology for Enhanced Transdermal Drug Delivery. *Int. J. Pharm. Sci.* **2026**, *4*, 59–75. [CrossRef]
16. Peréz-Salas, J.L.; Moreno-Jiménez, M.R.; Medina-Torres, L.; Rocha-Guzmán, N.E.; Bernad-Bernad, M.J.; González-Laredo, R.F.; Gallegos-Infante, J.A. Development and Characterization of Bigels for the Topical Delivery of Curcumin. *Sci. Pharm.* **2025**, *93*, 28. [CrossRef]
17. Ansari, A.; Verma, M.; Majhi, S. Nanoemulgel: A Comprehensive Review of Formulation Strategies, Characterization, Patents and Applications. *Micro Nanosyst.* **2025**, *17*, 12–26. [CrossRef]
18. Singh, V.K.; Banerjee, I.; Agarwal, T.; Pramanik, K.; Bhattacharya, M.K.; Pal, K. Guar gum and sesame oil based novel bigels for controlled drug delivery. *Colloids Surf. B Biointerfaces* **2014**, *123*, 582–592. [CrossRef]
19. Rehman, K.; Zulfakar, M.H. Novel fish oil-based bigel system for controlled drug delivery and its influence on immunomodulatory activity of imiquimod against skin cancer. *Pharm. Res.* **2017**, *34*, 36–48. [CrossRef]
20. Yi, H.; Kang, Y.; Chang, Y. Structural and rheological properties of bigels formed with xanthan gum hydrogel and lecithin/glycerol monostearate oleogel. *Int. J. Biol. Macromol.* **2025**, *306*, 141549. [CrossRef]
21. Milutinov, J.; Krstonošić, V.; Ćirin, D.; Pavlović, N. Emulgels: Promising Carrier Systems for Food Ingredients and Drugs. *Polymers* **2023**, *15*, 2302. [CrossRef]
22. Jain, A.; Kumar, P.; Verma, A.; Mohanta, B.C.; Ashique, S.; Pal, R.; Kumar, S.; Mishra, N. Emulgel: A Cutting Edge Approach for Topical Drug Delivery System. *Curr. Drug Res. Rev.* **2025**, *17*, 217–236. [CrossRef]
23. Francavilla, A.; Corradini, M.G.; Joye, I.J. Bigels as Delivery Systems: Potential Uses and Applicability in Food. *Gels* **2023**, *9*, 648. [CrossRef]
24. Shakouri, S.; Tehrani, M.M.; Koocheki, A.; Farhoosh, R.; Abdolshahi, A.; Shariatifar, N. Bigels as Novel Drug Delivery Systems: A Systematic Review on Efficiency and Influential Factors. *Curr. Rev. Clin. Exp. Pharmacol.* **2025**, *20*, 231–242. [CrossRef]
25. Bruno, E.; Lupi, F.R.; Mammolenti, D.; Mileti, O.; Baldino, N.; Gabriele, D. Emulgels Structured with Dietary Fiber for Food Uses: A Rheological Model. *Foods* **2022**, *11*, 3866. [CrossRef]
26. Sagiri, S.S.; Singh, V.K.; Kulanthaivel, S.; Banerjee, I.; Basak, P.; Battachrya, M.K.; Pal, K. Stearate organogel-gelatin hydrogel based bigels: Physicochemical, thermal, mechanical characterizations and in vitro drug delivery applications. *J. Mech. Behav. Biomed. Mater.* **2015**, *43*, 1–17. [CrossRef]
27. Satapathy, S.; Singh, V.; Sagiri, S.; Agarwal, T.; Banerjee, I.; Bhattacharya, M.; Kumar, N.; Pal, K. Development and characterization of gelatin-based hydrogels, emulsion hydrogels, and bigels: A comparative study. *J. Appl. Polym. Sci.* **2015**, *132*, 41502. [CrossRef]
28. Wakhet, S.; Singh, V.K.; Sahoo, S.; Sagiri, S.S.; Kulanthaivel, S.; Bhattacharya, M.K.; Kumar, N.; Banerjee, I.; Pal, K. Characterization of gelatin–agar based phase separated hydrogel, emulgel and bigel: A comparative study. *J. Mater. Sci. Mater. Med.* **2015**, *26*, 118. [CrossRef]
29. Mazurkevičiūtė, A.; Matulytė, I.; Ivaškienė, M.; Žilius, M. Assessment of Physical, Mechanical, Biopharmaceutical Properties of Emulgels and Bigel Containing Ciclopirox Olamine. *Polymers* **2022**, *14*, 2783. [CrossRef]
30. Shelke, O.; Kulkarni, A. Carbomer: A Comprehensive Review. *Inven. Rapid Pharm. Tech* **2016**, *1*, 1–8.
31. Mohamad Hamdi, N.A.; Azmi, N.A.; Mohd Sabari, N.H.; Harun, A.F.; Haris, M.S. An insight into the use and advantages of Carbopol in topical mucoadhesive drug delivery system: A systematic review. *J. Pharm.* **2023**, *3*, 53–65. [CrossRef]
32. Safitri, F.I.; Nawangsari, D.; Febrina, D. Overview: Application of Carbopol 940 in Gel. In Proceedings of the International Conference on Health and Medical Sciences, Yogyakarta, Indonesia, 30 June 2020–1 July 2020. [CrossRef]
33. Hussain, A.; Khan, G.M.; Shah, S.U.; Shah, K.U.; Rahim, N.; Wahab, A.; Rehman, A.U. Development of a novel ketoprofen transdermal patch: Effect of almond oil as penetration enhancers on in-vitro and ex-vivo penetration of ketoprofen through rabbit skin. *Pak. J. Pharm. Sci.* **2012**, *25*, 227–232.
34. Kasparaviciene, G.; Maslii, Y.; Herbina, N.; Kazlauskiene, D.; Marksa, M.; Bernatoniene, J. Development and Evaluation of Two-Phase Gel Formulations for Enhanced Delivery of Active Ingredients: Sodium Diclofenac and Camphor. *Pharmaceutics* **2024**, *16*, 366. [CrossRef]
35. Said dos Santos, R.; Rosseto, H.C.; Bassi da Silva, J.; Vecchi, C.F.; Wilker Caetano, W.; Bruschi, M.L. The effect of carbomer 934P and different vegetable oils on physical stability, mechanical and rheological properties of emulsion-based systems containing propolis. *J. Mol. Liq.* **2020**, *307*, 112969. [CrossRef]
36. Said dos Santos, R.; Bassi da Silva, J.; Rosseto, H.C.; Vecchi, C.F.; Campanholi, K.D.S.S.; Caetano, W.; Bruschi, M.L. Emulgels Containing Propolis and Curcumin: The Effect of Type of Vegetable Oil, Poly(Acrylic Acid) and Bioactive Agent on Physicochemical Stability, Mechanical and Rheological Properties. *Gels* **2021**, *7*, 120. [CrossRef]
37. Botella-Martínez, C.; Pérez-Álvarez, J.Á.; Sayas-Barberá, E.; Fernández-López, J.; Viuda-Martos, M. Assessment of Chemical, Physicochemical, and Lipid Stability Properties of Gelled Emulsions Elaborated with Different Oils Chia (*Salvia hispanica* L.) or Hemp (*Cannabis sativa* L.) and Pseudocereals. *Foods* **2021**, *10*, 1463. [CrossRef]
38. Kanoujia, J.; Nikita; Parashar, P.; Singh, N.; Saraf, S.A. Tea tree and jojoba oils enriched bigel loaded with isotretinoin for effective management of acne. *Indian J. Nat. Prod. Resour.* **2021**, *12*, 158–163. [CrossRef]

39. Ilomuanya, M.O.; Hameedat, A.T.; Akang, E.N.; Ekama, S.O.; Silva, B.O.; Akanmu, A.S. Development and evaluation of mucoadhesive bigel containing tenofovir and maraviroc for HIV prophylaxis. *Future J. Pharm. Sci.* **2020**, *6*, 81. [CrossRef]
40. Lupi, F.R.; Gabriele, D.; Seta, L.; Baldino, N.; de Cindio, B.; Marino, R. Rheological investigation of pectin-based emulsion gels for pharmaceutical and cosmetic uses. *Rheol. Acta* **2015**, *54*, 41–52. [CrossRef]
41. Lupi, F.R.; Gentile, L.; Gabriele, D.; Mazzulla, S.; Baldino, N.; de Cindio, B. Olive oil and hyperthermal water bigels for cosmetic uses. *J. Colloid Interface Sci.* **2015**, *459*, 70–78. [CrossRef]
42. Rawat, A.; Gupta, S.S.; Kalluri, H.; Lowenborg, M.; Bhatia, K.; Warner, K. Rheological Characterization in the Development of Topical Drug Products. In *The Role of Microstructure in Topical Drug Product Development*; Langley, N., Michniak-Kohn, B., Osborne, D.W., Eds.; Springer International Publishing: Cham, Switzerland, 2019; pp. 3–45. [CrossRef]
43. Dong, L.; Liu, C.; Cun, D.; Fang, L. The effect of rheological behavior and microstructure of the emulgels on the release and permeation profiles of Terpinen-4-ol. *Eur. J. Pharm. Sci.* **2015**, *78*, 140–150. [CrossRef]
44. Teaima, M.H.; Badawi, N.M.; Attia, D.A.; El-Nabarawi, M.A.; Elmazar, M.M.; Mousa, S.A. Efficacy of pomegranate extract loaded solid lipid nanoparticles transdermal emulgel against Ehrlich ascites carcinoma. *Nanomedicine* **2022**, *39*, 102466. [CrossRef]
45. Andonova, V.Y.; Peneva, P.T.; Apostolova, E.G.; Dimcheva, T.D.; Peychev, Z.L.; Kassarova, M.I. Carbopol hydrogel/sorbitan monostearate-almond oil based organogel biphasic formulations: Preparation and characterization of the bigels. *Trop. J. Pharm. Res.* **2017**, *16*, 1455–1463. [CrossRef]
46. Peneva, P.; Andonova, V.; Dimcheva, T.; Kassarova, M. Technological and biopharmaceutical characterization of carbopol-based ketoprofen emulgels. *Indian J. Pharm. Educ. Res.* **2018**, *52*, 212–217.
47. Redkar, M.; Hassan, P.A.; Aswal, V.; Devarajan, P. Onion Phases of PEG-8 Distearate. *J. Pharm. Sci.* **2007**, *96*, 2436–2445. [CrossRef]
48. Müller, S.; Börschig, C.; Gronski, W.; Schmidt, C.; Roux, D. Shear-induced states of orientation of the lamellar phase of C12E4/Water. *Langmuir* **1999**, *15*, 7558–7564. [CrossRef]
49. Caboi, F.; Monduzzi, M. Didodecyldimethylammonium bromide vesicles and lamellar liquid crystals. A multinuclear NMR and optical microscopy study. *Langmuir* **1996**, *12*, 3548–3556. [CrossRef]
50. Jibry, N.; Heenan, R.K.; Murdan, S. Amphiphilogels for drug delivery: Formulation and characterization. *Pharm. Res.* **2004**, *21*, 1852–1861. [CrossRef]
51. Heertje, I.; Roijers, E.C.; Hendrickx, H.A.C.M. Liquid Crystalline Phases in the Structuring of Food Products. *LWT-Food Sci. Technol.* **1998**, *31*, 387–396. [CrossRef]
52. Mustan, F.; Politova-Brinkova, N.; Rossetti, D.; Rayment, P.; Tcholakova, S. Oil soluble surfactants as efficient foam stabilizers. *Colloids Surf. A Physicochem. Eng. Asp.* **2022**, *633*, 127874. [CrossRef]
53. Bandyopadhyay, P.; Neeta, N.S. Evidence for vesicle formation from 1:1 nonionic surfactant Span 60 and fatty alcohol mixtures in aqueous ethanol: Potential delivery vehicle composition. *Colloids Surf. B Biointerfaces* **2007**, *58*, 305–308. [CrossRef]
54. Mason, T.G.; Bibette, J.; Weitz, D.A. Yielding and flow of monodisperse emulsions. *J. Colloid Interface Sci.* **1996**, *179*, 439–448. [CrossRef]
55. Hyun, K.; Kim, S.H.; Ahn, K.H.; Lee, S.G. Large amplitude oscillatory shear as a way to classify the complex fluids. *J. Non-Newton. Fluid Mech.* **2002**, *107*, 51–65. [CrossRef]
56. Piau, J.M. Carbopol gels: Elastoviscoplastic and slippery glasses made of individual swollen sponges: Meso- and macroscopic properties, constitutive equations and scaling laws. *J. Non-Newton. Fluid Mech.* **2007**, *144*, 1–29. [CrossRef]
57. Dabbaghi, M.; Namjoshi, S.; Panchal, B.; Grice, J.E.; Prakash, S.; Roberts, M.S.; Mohammed, Y. Viscoelastic and Deformation Characteristics of Structurally Different Commercial Topical Systems. *Pharmaceutics* **2021**, *13*, 1351. [CrossRef]
58. A-sasutjarit, R.; Sirivat, A.; Vayumhasuwan, P. Viscoelastic properties of Carbopol 940 gels and their relationships to Piroxicam diffusion coefficients in gel bases. *Pharm. Res.* **2005**, *22*, 2134–2140. [CrossRef]
59. Berdey, I.I.; Voyt, O.I. Rheological properties of emulgel formulations based on different gelling agent. *Pharm. Innov. J.* **2016**, *5*, 76–79.
60. Yoshimura, A.S.; Prud'homme, R.K. Response of an elastic Bingham fluid to oscillatory shear. *Rheol. Acta* **1987**, *26*, 428–436. [CrossRef]
61. Batheja, P.; Sheihet, L.; Kohn, J.; Singer, A.J.; Michniak-Kohn, B. Topical drug delivery by a polymeric nanosphere gel: Formulation optimization and in vitro and in vivo skin distribution studies. *J. Control. Release* **2011**, *149*, 159–167. [CrossRef]
62. Jaworski, Z.; Spychaj, T.; Story, A.; Story, G. Carbomer microgels as model yield-stress fluids. *Rev. Chem. Eng.* **2021**, *38*, 881–919. [CrossRef]
63. Kim, J.Y.; Song, J.Y.; Lee, E.J.; Park, S.K. Rheological properties and microstructures of Carbopol gel network system. *Colloid Polym. Sci.* **2003**, *281*, 614–623. [CrossRef]
64. Li, S.; Luo, M.; Boldianu, A.B.; McClements, D.J. Food-Grade Emulsion Gels as Nutrient Delivery Systems—Standardized Workflow for Fabrication, Characterization, and Application. *Gels* **2026**, *12*, 298. [CrossRef]

65. Mata-Mota, J.D.; Gallegos-Infante, J.A.; Pérez-Martínez, J.D.; Rocha-Guzmán, N.E.; González-Laredo, R.F. Effect of hydrogel/oleogel ratio, speed and time of mixing, on the mechanical properties of bigel materials and the application of Cox-Merz rule. *Food Mater. Res*. **2023**, *3*, 24. [CrossRef]
66. González-Ulloa, G.; Jiménez-Rosado, M.; Rafii-El-Idrissi Benhnia, M.; Romero, A.; Ruiz-Mateos, E.; Ostos, F.J.; Perez-Puyana, V. Hybrid polymeric Hydrogel-based biomaterials with potential applications in regenerative medicine. *J. Mol. Liq*. **2023**, *384*, 122224. [CrossRef]
67. Li, C.; Liu, C.; Liu, J.; Fang, L. Correlation between rheological properties, in vitro release, and percutaneous permeation of tetrahydropalmatine. *AAPS PharmSciTech* **2011**, *12*, 1002–1010. [CrossRef]
68. Budai, L.; Budai, M.; Fülöpné Pápay, Z.E.; Vilimi, Z.; Antal, I. Rheological Considerations of Pharmaceutical Formulations: Focus on Viscoelasticity. *Gels* **2023**, *9*, 469. [CrossRef]
69. Al-Barghouthy, E.Y.; Hamed, S.; Mehyar, G.F.; AlKhatib, H.S. Comparative Evaluation of Spreadability Measurement Methods for Topical Semisolid Formulations/A Scoping Review. *Gels* **2025**, *11*, 1006. [CrossRef]
70. Calienni, M.N.; Martínez, L.M.; Izquierdo, M.C.; Alonso, S.d.V.; Montanari, J. Rheological and Viscoelastic Analysis of Hybrid Formulations for Topical Application. *Pharmaceutics* **2023**, *15*, 2392. [CrossRef]
71. Huang, N. Rheological Characterization of Pharmaceutical and Cosmetic Formulations for Cutaneous Applications. *Curr. Pharm. Des*. **2019**, *25*, 2349–2363. [CrossRef]
72. Simões, A.; Miranda, M.; Cardoso, C.; Veiga, F.; Vitorino, C. Rheology by Design: A Regulatory Tutorial for Analytical Method Validation. *Pharmaceutics* **2020**, *12*, 820. [CrossRef]

Disclaimer/Publisher's Note: The statements, opinions and data contained in all publications are solely those of the individual author(s) and contributor(s) and not of MDPI and/or the editor(s). MDPI and/or the editor(s) disclaim responsibility for any injury to people or property resulting from any ideas, methods, instructions or products referred to in the content.